# Systematic Study of the Thermophysical Properties of Imidazolium-Based Ionic Liquids with Cyano-Functionalized Anions

**7 AUTHORS,** INCLUDING:

Joao A. P. Coutinho
University of Aveiro
**482** PUBLICATIONS **12,290** CITATIONS

SEE PROFILE

Isabel Marrucho
New University of Lisbon
**250** PUBLICATIONS **6,964** CITATIONS

SEE PROFILE

Jose Nuno A Canongia Lopes
Technical University of Lisbon
**179** PUBLICATIONS **8,341** CITATIONS

SEE PROFILE

Mara G Freire
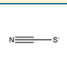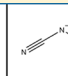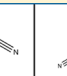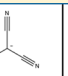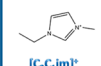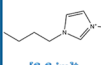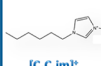University of Aveiro
**174** PUBLICATIONS **5,515** CITATIONS

SEE PROFILE

# Systematic Study of the Thermophysical Properties of Imidazolium-Based Ionic Liquids with Cyano-Functionalized Anions

Catarina M. S. S. Neves,[†] Kiki Adi Kurnia,[†] João A. P. Coutinho,[†] Isabel M. Marrucho,[†,‡]
José N. Canongia Lopes,[§] Mara G. Freire,*[,†,‡] and Luís Paulo N. Rebelo[‡]

[†]Departamento de Química, CICECO, Universidade de Aveiro, 3810-193 Aveiro, Portugal
[‡]Instituto de Tecnologia Química e Biológica, UNL, Avenida República, Apartado 127, 2780-901 Oeiras, Portugal
[§]Centro de Química Estrutural, Instituto Superior Técnico, 1049-001 Lisboa, Portugal

**S** *Supporting Information*

**ABSTRACT:** In the past few years, ionic liquids (ILs) with cyano-functionalized anions have shown to be improved candidates for electrochemical and separation applications. Nevertheless, only scattered data exist hitherto and a broad analysis of their structure−property relationship has yet to be attempted. Therefore, in this work, a systematic study of the densities, viscosities and refractive indices of imidazolium-based ILs with cyano-functionalized anions was carried out at 0.1 MPa within a broad temperature range (from 278 to 363 K). The ILs under study are based on 1-alkyl-3-methylimidazolium cations (alkyl = ethyl, butyl and hexyl) combined with the $[SCN]^-$, $[N(CN)_2]^-$, $[C(CN)_3]^-$ and $[B(CN)_4]^-$ anions. The selected matrix of cation/anion combinations allows us to provide a detailed and comprehensive investigation of the influence of the −CN group



through an analysis of the thermophysical properties of the related ILs. The results show that, regardless of the cation, the densities decrease with an increase in the number of cyano groups or anion molecular weight. Moreover, for a fixed cation and temperature, the refractive index of the ILs decreases according to the rank: $[SCN]^- > [N(CN)_2]^- \approx [C(CN)_3]^- > [B(CN)_4]^-$. On the other hand, no clear trend was observed for the viscosity of ILs and the respective number of −CN groups. The viscosity dependence on the cyano-functionalized anions decreases in the order: $[SCN]^- > [B(CN)_4]^- > [N(CN)_2]^- > [C(CN)_3]^-$. The isobaric thermal expansion coefficient, the derived molar refraction, the free volume, and the viscosity energy barrier of all compounds were estimated from the experimental data and are presented and discussed. Finally, group contribution models were applied, and new group contribution parameters are presented, extending these methods to the prediction of the ILs properties.

## ■ INTRODUCTION

Ionic liquids (ILs) have received enormous attention during the past decade as replacement solvents for currently used volatile organic solvents.[1] Chemically, ILs are composed of bulky organic cations coupled either with organic or inorganic anions. Different combinations of their ions and the introduction of specific and functionalized groups lead to significant changes in their thermophysical properties and phase behavior and, therefore, ILs have been labeled as "designer solvents" and "task-specific fluids". ILs thus provide the scientific community a plethora of research opportunities for exploring their unique and interesting properties. Most of the ILs studied to date present negligible volatility and nonflammability; this combination has made a crucial contribution toward their selection for a large range of applications.

One of the severest barriers to the industrial application of ILs is the relatively high viscosities of some fluids compared to those of molecular organic solvents, a fact that leads to lower mass transfer coefficients and higher energy requirements. Hence, the search for new and more versatile ILs is also being driven by the need for low viscosity materials. A considerable amount of work focusing on ILs containing fluoride-based anions has been published, particularly due to their low viscosity coupled with high thermal stability.[2−4] However, ILs with cyano-functionalized anions are a set of fluids that have been somewhat underexplored despite their remarkably low viscosities.

In 2001, MacFarlane et al.[5] reported the synthesis of novel ILs containing the dicyanamide anion − exceptional fluids with low melting temperatures and significantly low viscosities. Although this finding was shown more than a decade ago, the subsequent studies of the application of ILs with −CN groups have mostly centered on their use as electrolytes and in dye-sensitized solar cells prompted by the observation that these anions can produce some of the most fluid and conductive ILs.[6−9] More recently, this type of ILs has also been tested in

**Figure 1.** Ionic structures and cation−anion matrix of the studied ILs: ●, ILs studied; ○, ILs not studied.

separation approaches, such as supported IL membranes (SILM) for the selective separation of $CO_2$ and $N_2$,[10] stationary phases in chromatographic techniques,[11] and in the recovery of *n*-butanol from aqueous media.[12] In addition, when dealing with liquid−liquid extractive systems, Neves et al.[13] proposed the use of phosphonium-based ILs with cyano-functionalized anions for the improved separation of ethanol and water mixtures. Meindersma and co-workers[14] evaluated a large number of ILs for the extraction of aromatic compounds from their mixtures with aliphatic hydrocarbons. Remarkably, from the 121 evaluated ILs, only four compounds provided high mass-based distribution coefficients with selectivities comparable to or higher than those observed with sulfolane, all of which are cyano-based fluids.[14] ILs with −CN-based anions are also good candidates both to extract added-value compounds found in biomass, such as phenolic compounds,[15] and to dissolve carbohydrates and sugar alcohols,[16] a point which implies promising applications in biorefinery processes.

To fully optimize the wide range of applications where ILs with cyano-functionalized anions are superior candidates, the knowledge of their reliable thermophysical properties is of foremost importance. A number of reports concerning the thermophysical properties of scattered ILs with −CN-based anions are available in the literature.[17−51] Nevertheless, an extensive and comprehensive characterization of a cation−anion matrix capable of providing a consistent understanding of structure−property relationships has not yet been attempted. Therefore, this project was carried out to systematically characterize imidazolium-based ILs with cyano-functionalized anions. 1-Alkyl-3-methylimidazolium cations combined with progressively −CN-functionalized anions ([SCN]⁻, [N-(CN)₂]⁻, [C(CN)₃]⁻ and [B(CN)₄]⁻) permit a general overview of the changes that occur in their thermophysical properties, namely density, viscosity, and refractive index, as well as the dependence of all properties on temperature. The cation−anion matrix of the ILs studied is schematically shown in Figure 1.

Based on the experimental data and other literature results,[17−50] novel group contribution parameters for the Gardas and Coutinho models[51,52] are proposed here for all the −CN-functionalized anions aiming at predicting densities,

viscosities, and refractive indices of ILs not previously investigated experimentally.

## ■ EXPERIMENTAL SECTION

**Materials.** Nine imidazolium-based ILs containing anions with −CN groups, namely, 1-ethyl-3-methylimidazolium thiocyanate, [C₂C₁im][SCN] (mass fraction purity >98%), 1-butyl-3-methylimidazolium thiocyanate, [C₄C₁im][SCN] (mass fraction purity >98%), 1-ethyl-3-methylimidazolium dicyanamide, [C₂C₁im][N(CN)₂] (mass fraction purity >98%), 1-butyl-3-methylimidazolium dicyanamide, [C₄C₁im][N(CN)₂] (mass fraction purity >98%), 1-hexyl-3-methylimidazolium dicyanamide, [C₆C₁im][N(CN)₂] (mass fraction purity >98%), 1-ethyl-3-methylimidazolium tricyanomethane, [C₂C₁im][C(CN)₃] (mass fraction purity >98%), 1-butyl-3-methylimidazolium tricyanomethane, [C₄C₁im][C(CN)₃] (mass fraction purity >98%), 1-ethyl-3-methylimidazolium tetracyanoborate, [C₂C₁im][B(CN)₄] (mass fraction purity >98%), and 1-hexyl-3-methylimidazolium tetracyanoborate, [C₆C₁im][B(CN)₄] (mass fraction purity >98%), were studied from the perspective of understanding their structure−property relationships. Two tetrafluoroborate-based ILs, namely, 1-ethyl-3-methylimidazolium tetrafluoroborate, [C₂C₁im][BF₄] (mass fraction purity >99%), and 1-butyl-3-methylimidazolium tetrafluoroborate, [C₄C₁im][BF₄] (mass fraction purity >99%), were also used to validate the novel data as well as to compare with the results obtained for the −CN-containing ILs.

All the [SCN]-, [N(CN)₂]-, and [BF₄]-based compounds were acquired at Iolitec, whereas the [C(CN)₃]- and [B(CN)₄]-based fluids were kindly offered by Merck KGaA Germany.

Prior to the experimental measurements, all samples were dried and purified under constant stirring, high vacuum (10⁻⁵ Pa) and moderate temperature (353 K) for at least 48 h. The purity of each IL was further evaluated by ¹H and ¹³C NMR and was found to be in accordance with the levels given by the suppliers. All the ILs under studied are hygroscopic and their water content, before and after the experimental determinations, was determined using a Metrohm 831 Karl Fischer coulometer. The water content was found to be below 300 ppm for all samples and no significant water adsorption occurred
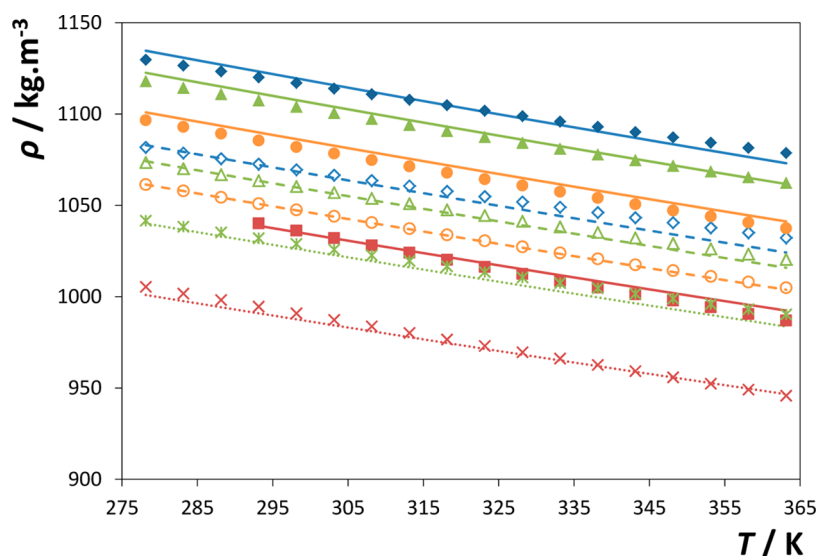
10272

dx.doi.org/10.1021/jp405913b | *J. Phys. Chem. B* 2013, 117, 10271−10283

**Figure 2.** Experimental density data as a function of temperature, and at 0.1 MPa, for the $[C_2C_1im]$-, $[C_4C_1im]$- and $[C_6C_1im]$-based ILs (filled symbols, empty symbols, and crosses, respectively) and respective prediction with the Gardas and Coutinho group contribution method[52] (full, dashed, and dotted lines, respectively): ♦, $[SCN]^-$; ▲, ∗, $[N(CN)_2]^-$; ●, $[C(CN)_3]^-$; ■, ×, $[B(CN)_4]^-$.

during the experimental measurements. The analyte used for the coulometric Karl Fischer titration was Hydranal - Coulomat AG from Riedel-de Haën.

**Experimental Procedure.** After drying, the densities ($\rho$) and viscosities ($\eta$) of all ILs were measured at pressures close to ambient pressure, ≈ 0.1 MPa, and in the temperature range from (278.15 to 363.15) K, using an automated SVM 3000 Anton Paar rotational Stabinger viscometer-densimeter. Further details regarding the operation system can be found elsewhere.[18,22] The uncertainty in temperature is ±0.02 K, the relative uncertainty for the dynamic viscosity is ±0.35%, and the absolute uncertainty for the density is ±5 × 10$^{-4}$ g·cm$^{-3}$. The refractive indices ($n_D$) were measured at 589.3 nm, at ≈0.1 MPa, and in the temperature range from (278.15 to 363.15) K, using an Anton Paar Abbemat 500 Refractometer developed for measuring both liquid and solid samples. At least seven measurements were taken for each sample and at each temperature to ensure the effectiveness of the measurements. The associated uncertainty to the refractive index is within 2 × 10$^{-5}$ $n_D$. Previous data for other ILs are published elsewhere and support the viability of the equipment to determine accurate refractive indices of IL samples.[53,54]

It should be pointed out that the properties associated with $[C_2C_1im][B(CN)_4]$ were studied in a narrower temperature range, from 293.15 to 363.15 K, due to the fact that its melting temperature is ca. 286 K.

## ■ RESULTS AND DISCUSSION

**Density.** The experimental density data for all the room temperature ILs with anions with −CN groups are depicted in Figure 2 and reported in Table S1, in the Supporting Information. The densities are provided in 5 K intervals and from 278.15 to 363.15 K, with the exception of $[C_2C_1im][B(CN)_4]$. The experimental data of the $[BF_4]$-based fluids are also presented in Table S1 for comparison purposes.

The comparison between the data obtained in this work and those already reported in literature is shown in the Supporting Information (Figures S1−S5). In addition to the measurement of the CN-based ILs, we also measured the density of two well-

studied compounds, namely $[C_2C_1im][BF_4]$ and $[C_4C_1im]$-$[BF_4]$. For $[C_2C_1im][BF_4]$ and $[C_4C_1im][BF_4]$, an average relative deviation of 0.028% and 0.014%, respectively, between our data and those previously reported was found.

For the ILs containing the cyano-functionalized anions, where fewer literature data exist, the average relative deviation between our data and those previously published[17−50] is within 1%. Two main exceptions were found for the data reported by Schreiner et al.[32] and Yoshida et al.[41] where higher relative deviations were observed for the ILs $[C_2C_1im][N(CN)_2]$ and $[C_2C_1im][C(CN)_3]$. These higher deviations may be attributable either to the purity of the samples that were synthesized by the authors[32,41] or to the use of a different experimental setup such as a pycnometer.[41] Nevertheless, and in general, the density data obtained in this work are in good agreement with most of the published results.[17−50]

Figure 2 presents density as a function of temperature for the −CN-functionalized ILs under study. In all samples, the density values decrease with increasing temperature.

For both fluoride-based or −CN-containing anions, the densities of the ILs decrease with the increase in the alkyl side chain length in the imidazolium cation. Accordingly, at a fixed temperature, the densities of the cation can be ranked in the following order: $[C_2C_1im]^+ > [C_4C_1im]^+ > [C_6C_1im]^+$. This trend is in agreement with previous investigations making use of ILs containing 1-alkyl-3-methylimidazolium cations combined with different anions.[43,55−57]

In fact, the decrease in density along the $[C_nC_1im]^+$ series corresponds to a regular and well-defined increase in the molar volume of the corresponding ILs as their alkyl side chains increase in length. It was originally demonstrated by Rebelo and co-workers[58,59] that such a trend is independent of the IL anion, and at 298.15 K the addition of one methylene group (−CH$_2$−) to the alkyl side chain increases the IL molar volume by a constant value of 17.1 ± 0.3 cm$^3$·mol$^{-1}$. Later, this concept was found to be valid also for the addition of methylene groups to the alkyl side chains of some anions such as alkylsulfonate or alkylsulfate.[59]

Taking into account the ideas expressed in the previous paragraph, we have decided to test the molar volume

10273

dx.doi.org/10.1021/jp405913b | J. Phys. Chem. B 2013, 117, 10271−10283

interadditive character of the cyano-based $[C_nC_1im][X(CN)_m]$ series, with $n = 2$, 4, or 6 and $m = 1$ ($X = S$), 2 ($X = N$), 3 ($X = C$) or 4 ($X = B$). It must be stressed that the anions in this series are not completely homologous due to the presence of different central atoms.

Since we have experimental density data for all ILs within the series with $n = 2$ or $m = 2$ (based on the ethyl-methylimidazolium cation and the dicyanamide anion), we were able to calculate the differences according to

$$\Delta V_m(n) = V_m([C_nC_1im][N(CN)_2]) \\ - V_m([C_2C_1im][N(CN)_2]) \quad (1)$$

$$\Delta V_m(m) = V_m([C_nC_1im][X(CN)_m]) \\ - V_m([C_2C_1im][N(CN)_2]) \quad (2)$$

which further allow one to estimate the molar volumes of any of the ILs within the series,

$$V_m([C_nC_1im][X(CN)_m]) = V_m([C_2C_1im][N(CN)_2]) \\ + \Delta V_m(n) + \Delta V_m(m) \quad (3)$$

Figure 3 shows the experimental (filled circles) and estimated (empty circles) $V_m$ values in the $([C_nC_1im][X(CN)_m])$ series,
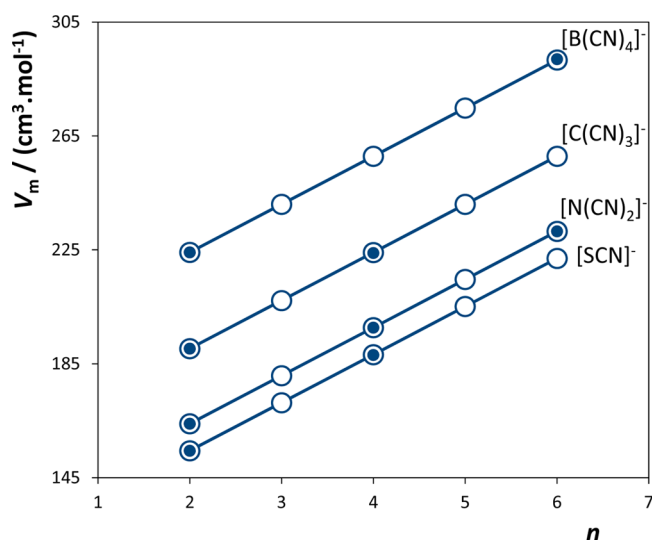


**Figure 3.** Experimental (●) and calculated (○) molar volumes at 333.15 K for the $([C_nC_1im][X(CN)_m])$ series (matrix), where $n$ is the number of carbons in the alkyl side chain of the cation, $m$ is the number of cyano groups in the anion and $X$ (S, N, C or B) is the anion central atom.

with $n = 2$ to 6 and $m = 1$ to 4 ($X = S$, N, C or B). The corresponding values are given in Table 1. The almost perfect overlap between the two sets of data—relative deviations always lower than 0.2%—demonstrate the high internal consistency of the density measurements and the additive character of the molar volumes within the series. Such behavior allows not only the prediction of other molar volume values within the series but also warrants the incorporation of this series in more general group-contribution molar volume prediction schemes.

For a fixed cation and at a common temperature, as expected, the [BF$_4$]-based ILs present higher density values than those based on the −CN anions due to the higher mass of the

**Table 1. Experimental and Calculated Molar Volumes ($V_m$(exp) and $V_m$(calc), Respectively) and Corresponding Relative Deviations for the ($[C_nC_1im][X(CN)_m]$) Series (Matrix) (cf. Figure 3 Caption)**

| T/K | ↓ cation / anion → | $V_m$(exp)/(cm³·mol⁻¹) | | | | $V_m$(calc)/(cm³·mol⁻¹) | | | | ($V_m$(calc) − $V_m$(exp))/$V_m$(exp) × 100 | | | |
|---|---|---|---|---|---|---|---|---|---|---|---|---|---|
| | | [SCN]⁻ | [N(CN)$_2$]⁻ | [C(CN)$_3$]⁻ | [B(CN)$_4$]⁻ | [SCN]⁻ | [N(CN)$_2$]⁻ | [C(CN)$_3$]⁻ | [B(CN)$_4$]⁻ | [SCN]⁻ | [N(CN)$_2$]⁻ | [C(CN)$_3$]⁻ | [B(CN)$_4$]⁻ |
| 289.15 | [C$_2$C$_1$im]⁺ | 151.57 | 160.56 | 186.04 | 218.22 | 151.57 | 160.56 | 186.04 | 218.22 | 0.00 | 0.00 | 0.00 | 0.00 |
| | [C$_4$C$_1$im]⁺ | 184.48 | 193.59 | 218.88 | -- | 184.59 | 193.59 | 219.07 | 251.25 | 0.06 | 0.00 | 0.08 | -- |
| | [C$_6$C$_1$im]⁺ | -- | 226.71 | -- | 284.69 | 217.71 | 226.71 | 252.19 | 284.37 | -- | 0.00 | -- | −0.11 |
| 333.15 | [C$_2$C$_1$im]⁺ | 154.48 | 163.98 | 190.35 | 224.15 | 154.48 | 163.98 | 190.35 | 224.15 | 0.00 | 0.00 | 0.00 | 0.00 |
| | [C$_4$C$_1$im]⁺ | 188.08 | 197.71 | 223.91 | -- | 188.21 | 197.71 | 224.08 | 257.88 | 0.07 | 0.00 | 0.08 | -- |
| | [C$_6$C$_1$im]⁺ | -- | 231.52 | -- | 292.00 | 222.03 | 231.52 | 257.90 | 291.70 | -- | 0.00 | -- | −0.10 |
| 363.15 | [C$_2$C$_1$im]⁺ | 156.95 | 166.86 | 194.02 | 229.10 | 156.95 | 166.86 | 194.02 | 229.10 | 0.00 | 0.00 | 0.00 | 0.00 |
| | [C$_4$C$_1$im]⁺ | 191.15 | 201.16 | 228.16 | -- | 191.24 | 201.16 | 228.32 | 263.39 | 0.05 | 0.00 | 0.07 | -- |
| | [C$_6$C$_1$im]⁺ | -- | 235.54 | -- | 298.27 | 225.63 | 235.54 | 262.70 | 297.78 | -- | 0.00 | -- | −0.16 |

fluorine atom. When analyzing the effect of the −CN groups, the densities decrease in the following order: $[SCN]^-$ > $[N(CN)_2]^-$ > $[C(CN)_3]^-$ > $[B(CN)_4]^-$. In summary, both the increase in the length of the aliphatic moiety in the cation and the increase in the number of −CN groups in the anion produces less dense ILs. In general, IL density decreases with the decrease in the ions' molecular weight of the −CN-based series studied here ($M_w([SCN]^-)$ = 58.08 g·mol$^{-1}$ < $M_w([N-(CN)_2]^-)$ = 66.04 g·mol$^{-1}$ < $M_w([C(CN)_3]^-)$ = 90.06 g·mol$^{-1}$ < $M_w([B(CN)_4]^-)$ = 114.88 g·mol$^{-1}$). In fact, there is a strict correlation between density and the anion molecular weight for the −CN-functionalized ILs as depicted in Figure 4. Never-
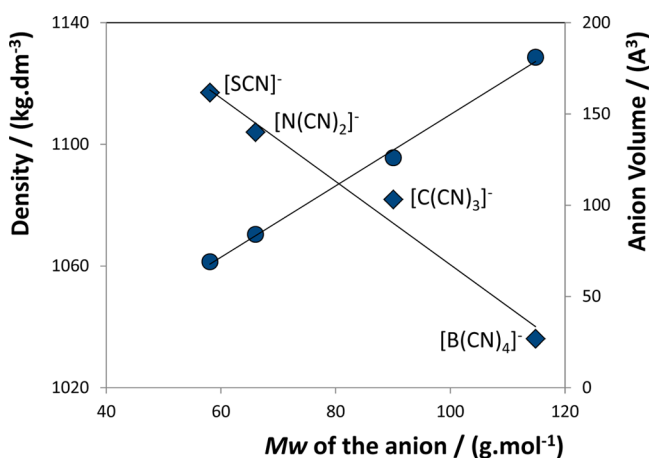


**Figure 4.** Density (♦) and anion volume determined by the Gardas and Coutinho group contributon model[52] (●) of $[C_2C_1im]$-based ILs at 298.15 K as a function of the anion molecular weight.

theless, this density dependence on the anion molecular weight is the opposite of that observed by Kolbeck et al.[60] with fluoride-based ILs, where an increase in the molecular weight of the anion (or number of fluorine atoms at the anion) results in denser fluids. Fluorine atoms are heavier than hydrogen, but about the same size. The introduction of fluorine atoms has little effect on the molecular size yet a strong influence on the molecular weight of a particular compound.

The density data measured in this work were also used to widen the group contribution parameter values in the extension of the Ye and Shreeve group contribution method[61] previously proposed by Gardas and Coutinho,[51] intended to enable the prediction of densities of ILs not experimentally addressed. The contributions of the −CN-based anions were estimated according to eq 4,

$$\rho = \frac{Mw}{NV(a + bT + cp)} \tag{4}$$

where $\rho$ is the density in kg·m$^{-3}$, $M_w$ is the IL molecular weight in kg·mol$^{-1}$, $N$ is the Avogadro constant, $V$ is the IL volume in m$^3$, $T$ is the temperature in K, and $p$ is the pressure in MPa. The coefficients $a$, $b$, and $c$ were previously proposed[51] using a broad set of experimental data and using the values of 0.8005 ± 0.0002, (6.652 ± 0.007) × 10$^{-4}$ K$^{-1}$ and (−5.919 ± 0.024) × 10$^{-4}$ MPa$^{-1}$, respectively.

To obtain and propose novel group contribution parameters for the −CN-functionalized anions, both the experimental density values obtained in this work and those from the literature[17−50] were used to gather the most accurate values. The new proposed ionic volumes are given in Table 2 along

**Table 2. Ionic Volumes, $V$, Determined with the Gardas and Coutinho Group Contribution Model (within 278.15 and 363.15 K)[51]**

| ionic species | $V$ / Å$^3$ |
|---|---|
| Cation[51] | |
| $[C_1C_1im]^+$ | 154 |
| Anion | |
| $[SCN]^-$ | 69 |
| $[N(CN)_2]^-$ | 84 |
| $[C(CN)_3]^-$ | 126 |
| $[B(CN)_4]^-$ | 181 |
| Additional Group[51] | |
| −CH$_2$ | 28 |

with those previously reported for the IL cation.[51] Although we had already proposed ionic volumes for some of the investigated anions,[18,22] the most accurate values are those reported in this work since the highest density databank was compiled here.

Figure 2 compares the experimental density data with the predicted density values based on the group contribution method[51] and their dependence on temperature. The dependence of density on temperature is, in general, well described, and the predicted values are in good agreement with the experimental data. A maximum absolute average deviation of 0.59% for the 509 reported density data points was found.

Figure 3 depicts the dependence of the predicted anion volume by the Gardas and Coutinho group contribution model[51] along with the molecular weight of the anion showing again a strict dependence on both properties for structurally similar ILs. An increase in the ionic volume of the −CN-functionalized anions results in denser fluids.

The isobaric thermal expansion coefficients ($\alpha_p$), which consider the volumetric changes with temperature, were calculated from the fitting of the experimental data using eq 5,

$$\alpha_P = -\frac{1}{\rho}\left(\frac{\partial \rho}{\partial T}\right)_P = -\left(\frac{\partial \ln \rho}{\partial T}\right)_P \tag{5}$$

where $\rho$ is the density in kg·m$^{-3}$, $T$ is the temperature in K and $\rho$ is the pressure in MPa.

Despite the controversy surrounding the application of a linear correlation or a second order polynomial equation to describe the experimental density data, we found the use of a linear function in $T$ to be adequate to describe the experimental density data (at least in the temperature range investigated in this work). Furthermore, the use of a linear regression implies that the thermal expansion coefficient values are constant at a given pressure.

In Table 3, $\alpha_p$ is presented for all the investigated ILs at a common temperature of 298.15 K. Among the set of cyano-containing ILs, the thermal expansion coefficients are very close and vary between (5.43−7.49) × 10$^{-4}$ K$^{-1}$ for $[C_2C_1im][SCN]$ and for $[C_2C_1im][B(CN)_4]$, respectively. These values are considerably lower than those of molecular organic solvents and higher than those of classical molten salts.[62] ILs containing a smaller alkyl chain present a lower expansion coefficient compared to those having a longer aliphatic moiety. This suggests that the large cation size of the ILs reduces electrostatic interactions and thus facilitates expansion. It seems, however, that the thermal expansion coefficients are less dependent on the cation alkyl side chain length than on the anion which constitutes a given IL, at least for the anion−cation

**Table 3. Fitting Parameters of Eq 5 and Thermal Expansion Coefficients, $\alpha_p$, in the Temperature Range from 278.15 to 263.15 K and at 0.1 MPa for the Studied ILs**

| ionic liquid | $10^4\,(\alpha_p \pm \sigma)/\mathrm{K}^{-1}$ |
|---|---|
| $[\mathrm{C_2C_1im}][\mathrm{SCN}]$ | $5.43 \pm 0.02$ |
| $[\mathrm{C_4C_1im}][\mathrm{SCN}]$ | $5.52 \pm 0.02$ |
| $[\mathrm{C_2C_1im}][\mathrm{N(CN)_2}]$ | $5.99 \pm 0.02$ |
| $[\mathrm{C_4C_1im}][\mathrm{N(CN)_2}]$ | $5.97 \pm 0.02$ |
| $[\mathrm{C_6C_1im}][\mathrm{N(CN)_2}]$ | $5.94 \pm 0.02$ |
| $[\mathrm{C_2C_1im}][\mathrm{C(CN)_3}]$ | $6.53 \pm 0.02$ |
| $[\mathrm{C_4C_1im}][\mathrm{C(CN)_3}]$ | $6.44 \pm 0.02$ |
| $[\mathrm{C_2C_1im}][\mathrm{B(CN)_4}]$ | $7.49 \pm 0.03$ |
| $[\mathrm{C_6C_1im}][\mathrm{B(CN)_4}]$ | $7.21 \pm 0.01$ |
| $[\mathrm{C_2C_1im}][\mathrm{BF_4}]$ | $5.90 \pm 0.02$ |
| $[\mathrm{C_4C_1im}][\mathrm{BF_4}]$ | $5.91 \pm 0.02$ |

combinations studied here. The expansion of the cyano-constituting anions is more dependent on temperature than the aliphatic moieties present in the imidazolium ring (from $[\mathrm{C_2C_1im}]^+$ to $[\mathrm{C_6C_1im}]^+$). An increase in the number of $-$CN groups, for a common cation such as $[\mathrm{C_2C_1im}]^+$, leads to an increase in the thermal expansion coefficient of the IL. In addition, when comparing the $[\mathrm{BF_4}]$- and $[\mathrm{B(CN)_4}]$-based ILs, there is evidence that the fluorinated ILs are less expansible than the cyano-based fluids.

**Viscosity.** Viscosity is an important property of ILs as it influences ionic conductivity and mass transport phenomena, thereby governing their suitability for particular applications. The experimental viscosity data for the ILs studied are reported in Table S2, in the Supporting Information, and depicted in Figure 5. The results indicate that the viscosity of the selected ILs decreases markedly with temperature increase. For instance, for the cyano-based compounds, a rise in temperature from 298.15 to 303.15 K, leads to a fall in viscosity from 14 to 22%. These values can be compared with a decrease in viscosity of 5% and 10% for $n$-hexane and water, respectively, in the same temperature range.[62]

The comparison between our experimental viscosity data and those reported in the literature is given in the Supporting Information (Figures S6–S10). Larger deviations are now observed in the viscosity data, as compared with the density results. Even for the well-studied $[\mathrm{BF_4}]$-based fluids, average relative deviations in the order of 2.50% are observed. For those ILs with $-$CN-containing anions average relative deviations ca. to 3.23% were detected.[17−50] The reasons for this high disparity among diverse authors are related to temperature control (since viscosity is highly temperature dependent), purity of the samples (including the preparation procedures), equipment used, and sample handling since the adsorption of water during the experiments is a crucial factor in determining accurate viscosity values.

The structural effects of the ILs toward their viscosity values are depicted in Figure 6.

At present, ILs with low viscosity are highly desirable for industrial applications. For all the investigated samples with a common anion, viscosity increases with the increase of the alkyl side chain length of the imidazolium cation according to $[\mathrm{C_6C_1im}]^+ > [\mathrm{C_4C_1im}]^+ > [\mathrm{C_2C_1im}]^+$. In general, lengthening the aliphatic moieties in ILs increases their viscosity through stronger van der Waals interactions, as observed for other imidazolium-based ILs combined with different anions.[3,54]

The viscosity results within the $([\mathrm{C_nC_1im}][X(\mathrm{CN})_m])$ series were also analyzed in terms of the possible existence of an additive behavior. As in the case of the density data (cf. above), the following differences were considered:

$$\Delta \ln \eta(n) = \ln \eta([\mathrm{C_nC_1im}][\mathrm{N(CN)_2}]) \\ - \ln \eta([\mathrm{C_2C_1im}][\mathrm{N(CN)_2}]) \tag{6}$$

$$\Delta \ln \eta(m) = \ln \eta([\mathrm{C_2C_1im}][X(\mathrm{CN})_m]) \\ - \ln \eta([\mathrm{C_2C_1im}][\mathrm{N(CN)_2}]) \tag{7}$$

and the viscosities of all ILs within the series were calculated via,
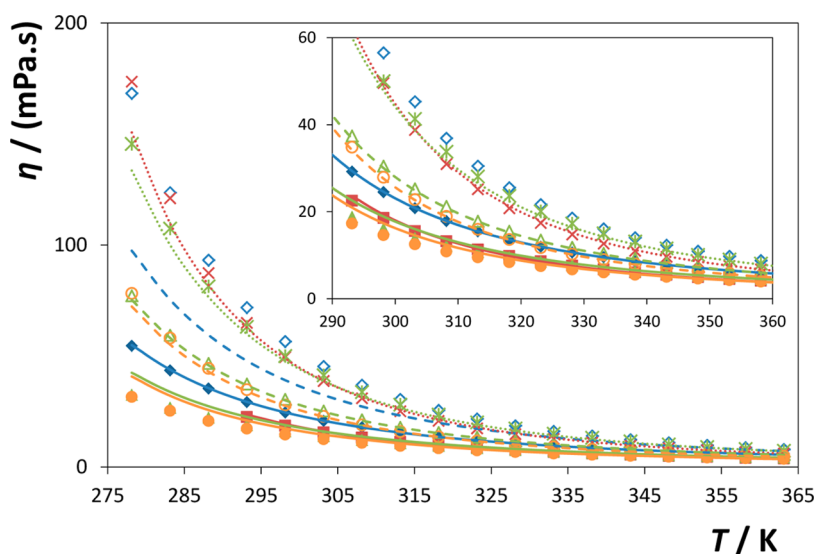


**Figure 5.** Experimental viscosity data as a function of temperature, and at 0.1 MPa, for the $[\mathrm{C_2C_1im}]$-, $[\mathrm{C_4C_1im}]$-, and $[\mathrm{C_6C_1im}]$-based ILs (filled symbols, empty symbols, and crosses, respectively) and respective prediction with the Gardas and Coutinho group contribution method[52] (full, dashed, and dotted lines, respectively): ♦, $[\mathrm{SCN}]^-$; ▲, ∗, $[\mathrm{N(CN)_2}]^-$; ●, $[\mathrm{C(CN)_3}]^-$; ■, ×, $[\mathrm{B(CN)_4}]^-$.
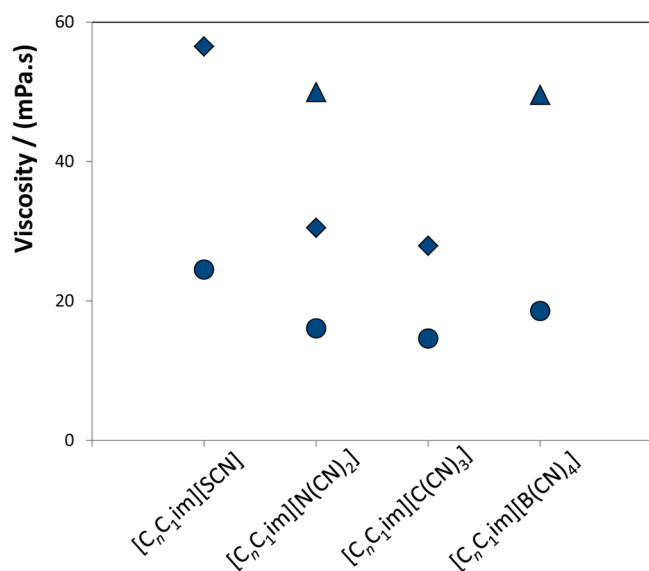
**Figure 6.** Viscosity at 298.15 K of cyano-functionalized anions combined with the cations: ●, $[C_2C_1im]^+$; ◆, $[C_4C_1im]^+$; ▲, $[C_6C_1im]^+$.

$$\ln \eta([C_nC_1im][X(CN)_m]) = \ln \eta([C_2C_1im][N(CN)_2]) + \Delta \ln \eta(n) + \Delta \ln \eta(m) \tag{8}$$

The use of $\ln\eta$ instead of $\eta$ values is warranted by the use of the Grunberg–Nissan model.[63]

The experimental and calculated results at fixed temperatures are presented in Table 4. Relative deviations up to 17% were observed, thus confirming that the ILs viscosity is not additive within the series.

For a common cation at a fixed temperature, the viscosity of the cyano-functionalized ILs decreases in the order $[SCN]^- > [B(CN)_4]^- > [N(CN)_2]^- > [C(CN)_3]^-$. This sequence is closely related to the intermolecular interactions that occur at the bulk liquid; however, a molecular-based understanding of the ionic liquids' dominating interactions is a challenging task. The high energy of cohesion, which increases with the increase of the ions size, induces the formation of viscous liquids if van der Waals interactions become predominant. It is also well-known that an increase in ion size reduces the electrostatic attraction inducing the formation of less viscous fluids. In cyano-based ILs there is no straight correlation between viscosity and anion molecular size, and it thus seems that there is a delicate balance between diverse interactions, which act in opposite ways. The ILs with an almost linear or flat shape and enhanced charge distribution anions, namely, $[N(CN)_2]^-$ and $[C(CN)_3]^-$, are the most fluid ILs investigated, notwithstanding their somewhat coordinating ability. Overall, for the cyano-functionalized ILs, an increase in anion size or in the number of −CN groups decreases the viscosity until $[C(CN)_3]^-$ whereas from $[C(CN)_3]^-$ to $[B(CN)_4]^-$ an opposite behavior is verified. It appears that the higher symmetry of the tetracyanoborate anion and its tetrahedral shape overlaps the decreasing tendency of viscosity as a function of the −CN number.

The $[BF_4]$-based fluids are more viscous than the cyano-containing compounds. The fluoride-based compounds have become compounds of election due to their low viscosities.[3] The higher charge distribution and lower polarizability of $[BF_4]^-$ contribute to reduced cohesive forces, van der Waals

**Table 4. Experimental and Calculated Viscosities ($\eta$(exp) and $\eta$(calc), Respectively) and Corresponding Relative Deviations for the ($[C_nC_1im][X(CN)_m]$) Series (Matrix) (cf. Figure 3 Caption)**

| T/K | ↓cation / anion→ | $\eta$(exp)/(mPa·s) | | | | $\eta$(calc)/(mPa·s) | | | | ($\eta$(calc) − $\eta$(exp))/$\eta$(exp) × 100 | | | |
|---|---|---|---|---|---|---|---|---|---|---|---|---|---|
| | | $[SCN]^-$ | $[N(CN)_2]^-$ | $[C(CN)_3]^-$ | $[B(CN)_4]^-$ | $[SCN]^-$ | $[N(CN)_2]^-$ | $[C(CN)_3]^-$ | $[B(CN)_4]^-$ | $[SCN]^-$ | $[N(CN)_2]^-$ | $[C(CN)_3]^-$ | $[B(CN)_4]^-$ |
| 289.15 | $[C_2C_1im]^+$ | 24.51 | 16.09 | 14.61 | 18.57 | 24.51 | 16.09 | 14.61 | 18.57 | 0.00 | 0.00 | 0.00 | 0.00 |
| | $[C_4C_1im]^+$ | 56.52 | 30.50 | 27.91 | -- | 46.45 | 30.50 | 27.69 | 35.19 | −17.81 | 0.00 | −0.77 | -- |
| | $[C_6C_1im]^+$ | -- | 49.99 | -- | 49.58 | 76.14 | 49.99 | 45.40 | 57.68 | -- | 0.00 | -- | 16.35 |
| 363.15 | $[C_2C_1im]^+$ | 5.48 | 4.23 | 3.66 | 3.81 | 5.48 | 4.23 | 3.66 | 3.81 | 0.00 | 0.00 | 0.00 | 0.00 |
| | $[C_4C_1im]^+$ | 7.93 | 5.67 | 4.83 | -- | 7.35 | 5.67 | 4.91 | 5.11 | −7.29 | 0.00 | 1.50 | -- |
| | $[C_6C_1im]^+$ | -- | 7.31 | -- | 6.09 | 9.48 | 7.31 | 6.33 | 6.59 | -- | 0.00 | -- | 8.17 |

interactions, and hydrogen-bonding, and thus to low viscous materials. Nevertheless, cyano-based ILs seem to overwhelm the typical low-viscosities displayed by fluorinated ILs. The outstandingly low viscosities of cyano-containing ILs, in particular the $[C(CN)_3]$-based compounds, make them especially appropriate for a wide range of applications.

The experimental viscosity data were correlated using the Vogel−Tammann−Fulcher model described in eq 9,

$$\ln \eta = A_\eta + \frac{B_\eta}{(T - C_\eta)} \qquad (9)$$

where $\eta$ is the viscosity in mPa·s, $T$ is the temperature in K, and $A_\eta$, $B_\eta$, and $C_\eta$ are adjustable parameters. The adjustable parameters were determined from the fitting of the experimental data and are presented in Table 5. The correlated viscosities are in good agreement with the experimental data with a maximum relative deviation of 0.18%.

**Table 5. Correlated Parameters $A_\eta$, $B_\eta$ and $C_\eta$ from the Vogel−Tammann−Fulcher Correlation Applied to the Experimental Data and the Derived Energy Barrier at 298.15 K**

| ionic liquid | $A_\eta/(\mathrm{mPa \cdot s})$ | $B_\eta/\mathrm{K}$ | $C_\eta/\mathrm{K}$ | $E_{298.15K}/(\mathrm{kJ \cdot mol^{-1}})$ |
|---|---|---|---|---|
| $[C_2C_1\mathrm{im}][SCN]$ | −1.4232 | 628.3 | 162.2 | 25.14 |
| $[C_4C_1\mathrm{im}][SCN]$ | −1.6841 | 710.7 | 173.8 | 33.99 |
| $[C_2C_1\mathrm{im}][N(CN)_2]$ | −1.4642 | 600.3 | 156.7 | 22.16 |
| $[C_4C_1\mathrm{im}][N(CN)_2]$ | −1.5729 | 637.0 | 170.5 | 28.91 |
| $[C_6C_1\mathrm{im}][N(CN)_2]$ | −1.7548 | 727.6 | 170.1 | 32.79 |
| $[C_2C_1\mathrm{im}][C(CN)_3]$ | −1.4582 | 535.9 | 168.7 | 23.65 |
| $[C_4C_1\mathrm{im}][C(CN)_3]$ | −1.5011 | 551.6 | 184.0 | 31.27 |
| $[C_2C_1\mathrm{im}][B(CN)_4]$ | −1.7288 | 586.2 | 172.1 | 27.26 |
| $[C_6C_1\mathrm{im}][B(CN)_4]$ | −1.7182 | 614.7 | 188.8 | 37.99 |
| $[C_2C_1\mathrm{im}][BF_4]$ | −1.5665 | 716.0 | 161.2 | 28.20 |
| $[C_4C_1\mathrm{im}][BF_4]$ | −2.0146 | 849.8 | 171.4 | 40.95 |

Since the high viscosity of ILs depends mainly on their intermolecular interactions such as H-bonding and dispersive and Coulombic interactions, an increase in temperature substantially decreases the intensity of H-bonding interactions, and consequently the viscosity of ILs largely decreases with temperature. The energy barrier of a fluid to shear stress, $E$, can be evaluated based on the viscosity dependence with temperature using the following equation:

$$E = R \cdot \frac{\partial(\ln \eta)}{\partial(1/T)} = R \cdot \left( \frac{B_\eta}{\left( \frac{C_\eta^2}{T^2} - \frac{2C_\eta}{T} + 1 \right)} \right) \qquad (10)$$

where $\eta$ is viscosity, $T$ is the temperature, $B_\eta$ and $C_\eta$ are the adjustable parameters obtained from eq 9, and $R$ is the universal gas constant.

The derived energy barriers at 298.15 K, $E_{298.15K}$, are listed in Table 5. Figure 7 depicts the energy barrier at 298.15 K and the absolute value of the pre-exponential coefficient of the Vogel−Tammann−Fulcher equation, $A_\eta$, as a function of the −CN-based anion.

Neither in the energy barrier values nor in the pre-exponential coefficient of the Vogel−Tammann−Fulcher equation are found straight patterns with the addition of −CN groups at the anion. The rates at which the fluidities of the ILs with different anions change with temperature provide
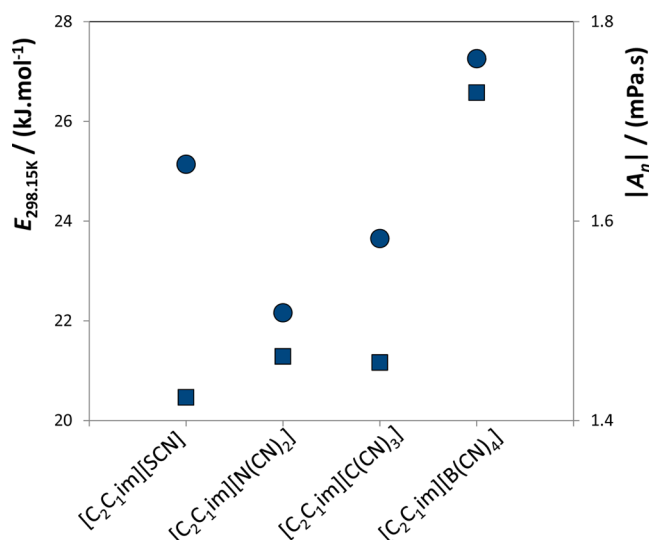


**Figure 7.** Energy barrier at 298.15 K (●) and absolute value of the pre-exponential coefficient of the Vogel−Tammann−Fulcher equation (■) of $[C_2C_1\mathrm{im}]$-based ILs.

information on the dynamics of particle motion in ILs. Thus, from the absolute values of the pre-exponential coefficient of the Vogel−Tammann−Fulcher equation, the dependence of viscosity on temperature, and therefore, the particles' motion ability in the fluid decreases in the order: $[C_2C_1\mathrm{im}][B(CN)_4]$ > $[C_2C_1\mathrm{im}][N(CN)_2]$ > $[C_2C_1\mathrm{im}][C(CN)_3]$ > $[C_2C_1\mathrm{im}][SCN]$. On the other hand, the energy barrier of the $[C_2C_1\mathrm{im}]$-based ILs decreases according to the following rank: $[B(CN)_4]^-$ > $[SCN]^-$ > $[C(CN)_3]^-$ > $[N(CN)_2]^-$. The higher the energy barrier value, the more difficult it is for the ions to move past each other. This can be a direct consequence of the size or entanglement of the ions and/or of the presence of stronger interactions in the fluid. Hence, the $[N(CN)_2]$-based fluids are the ILs that require less energy to move freely in the bulk, whereas the $[B(CN)_4]$-based ILs are those that need the most energy—possibly a result of their larger anion size and higher symmetry. In all examples shown in Table 5, the barrier energy increases with the size of the aliphatic moiety of the imidazolium ring. As explained before, ILs with longer alkyl side chain lengths also present stronger van der Waals interactions that overwhelm the cation−anion electrostatic interactions. Moreover, an increased molar volume in the cation can also inhibit the laminar flow.

The contribution of each CN-functionalized anion to the viscosity of the related ILs was further estimated using the group contribution method proposed by Gardas and Coutinho,[52] which makes use of the Vogel−Tammann−Fulcher model described in eq 9, and where $A_\eta$ and $B_\eta$ are obtained by a group contribution method according to

$$A_\eta = \sum_{i=1}^{k} n_i a_{i,\eta} \qquad (11)$$

$$B_\eta = \sum_{i=1}^{k} n_i b_{i,\eta} \qquad (12)$$

where $n_i$ is the number of groups of type $i$ and $k$ is the total number of different groups in the molecule.

The obtained parameters $a_{i\eta}$ and $b_{i\eta}$ are provided in Table 6 and allow us to predict viscosity values of novel ILs with similar

**Table 6. Group Contribution Parameters, $a_{i,\eta}$ and $b_{i,\eta}$, of the Group Contribution Method for the Prediction of Viscosity According to the Gardas and Coutinho Model[52]**

| ionic species | $a_{i,\eta}$ | $b_{i,\eta}/K$ |
|---|---|---|
| | Cation[52] | |
| $[C_1C_1im]^+$ | −7.271 | 510.51 |
| | Anions | |
| $[SCN]^-$ | −0.909 | 53.97 |
| $[N(CN)_2]^-$ | −1.204 | 58.16 |
| $[C(CN)_3]^-$ | −1.539 | 91.51 |
| $[B(CN)_4]^-$ | −1.737 | 132.16 |
| | Additional Group[52] | |
| $-CH_2$ | $-7.528 \times 10^{-2}$ | 40.92 |

anions. Some of these group contribution parameters had previously appeared in the literature,[52] although based on a more limited set of experimental data. The new groups proposed for the anions $[SCN]^-$, $[N(CN)_2]^-$, $[C(CN)_3]^-$, and $[B(CN)_4]^-$ were obtained making use of an extended database of experimental data (our experimental viscosity values together with experimental data reported in literature[17−50]). However, we continued to use the previously proposed value for $C_\eta$ of 165.06 K.[52] The predictive viscosity for the studied ILs is presented in Figure 5 together with the experimental data. The average relative deviation between the experimental data and the viscosity predicted by the Gardas and Coutinho model[52] was 9.71% for a total of 334 data points. Despite the large deviations, the cation alkyl side chain length and the anion nature effects on the viscosity values were always well predicted.
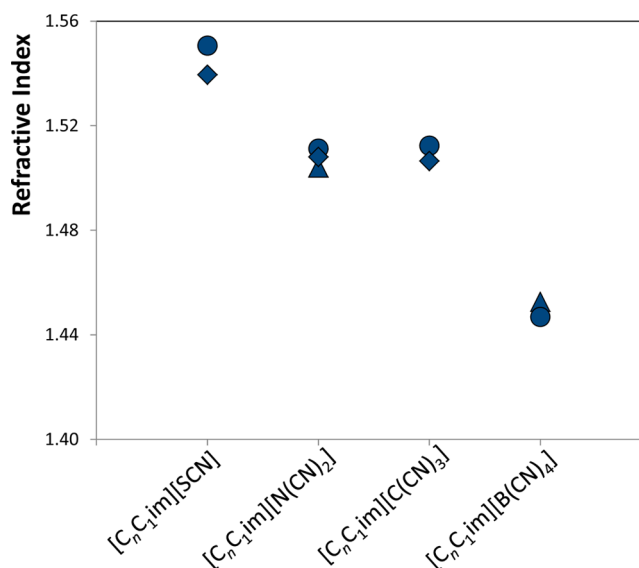
**Refractive Index.** The refractive index indicates the dielectric response to an electrical field induced by electromagnetic waves (light) and is thus an optical property of materials. The experimental refractive index data of the investigated ILs are listed in Table S3, in the Supporting Information, while Figure 8 presents a general overview of the results as a function of temperature. The refractive indices were measured within the range of temperatures from (283.15 to 353.15) K. As with the previous properties, the refractive index
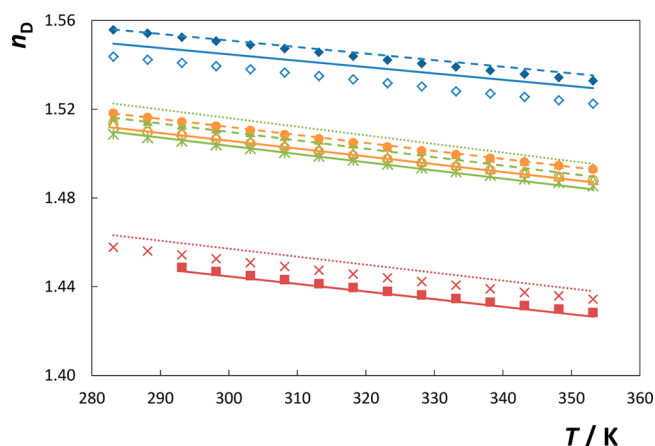


**Figure 8.** Experimental refractive index data as a function of temperature, and at 0.1 MPa, for the $[C_2C_1im]$-, $[C_4C_1im]$-, and $[C_6C_1im]$-based ILs (filled symbols, empty symbols, and crosses, respectively) and respective prediction with Gardas and Coutinho group contribution method[52] (full, dashed, and dotted lines, respectively): ♦, $[SCN]^-$; ▲, *, $[N(CN)_2]^-$; ●, $[C(CN)_3]^-$; ■, ×, $[B(CN)_4]^-$.

of $[C_2C_1im][B(CN)_4]$ was determined only above 293.15 K due to the higher melting temperature of this compound. In general, and for all the ILs under study, the refractive index decreased with an increase in temperature.

Refractive index data for ILs containing CN-functionalized anions are particularly scarce.[22,23,25,33,46] A comparison of our experimental data with published ones appears in the Supporting Information (Figures S11 and S12). In general, the values obtained here are in good agreement with the literature data, with an average relative deviation of 0.09%. Also for the $[BF_4]$-based fluids, a good agreement between our data and the published ones was observed with an average relative deviation of 0.06%.

An overall overview of the refractive index data at a fixed temperature of 298.15 K and according to the IL chemical structure is depicted in Figure 9.



**Figure 9.** Refractive Index at 298.15 K of cyano-functionalized anions combined with the cations: ●, $[C_2C_1im]^+$; ♦, $[C_4C_1im]^+$; ▲, $[C_6C_1im]^+$.

$[C_2C_1im][SCN]$ has the highest refractive index (1.55 at room temperature). In addition, most of the refractive indices of the cyano-functionalized ILs are higher than the liquid immersion oil commonly used in optical microscopy (1.51).[46] Therefore, the CN-based fluids can be envisaged as new and advantageous optical materials.

As previously reported,[22] the refractive indices of ILs are strongly dependent on the composing anion. For the cyano-constituting ILs, the refractive index decreases in the order $[SCN]^- > [N(CN)_2]^- \approx [C(CN)_3]^- > [B(CN)_4]^-$. Generally, the refractive index decreases with the anion molecular weight,[53] although an important exception is observed with the $[N(CN)_2]^-$ and $[C(CN)_3]^-$ anions which present similar values for a common cation. Usually, solvents with higher refractive indices, and hence large polarizability, should enjoy particularly strong dispersion forces, such as in the case of $[SCN]^-$ that presents a significant delocalization of charge. The refractive index data can be regarded as a measure of the relative extent of the apolar domains in the IL, and for a similar cation, the contribution of the $[N(CN)_2]^-$ and $[C(CN)_3]^-$ anions to these regimes is approximately the same. Among all

the studied ILs the $[BF_4]$-based fluids display the lowest refractive index values.

As a general rule, and since the refractive indices constitute a quantitative measure of the importance of the dispersive forces in the IL medium, it is expected that ILs with longer aliphatic moieties display higher refractive index values. This trend has been previously reported by Tariq et al.[55] for a large series of 1-alkyl-3-methylimidazolium-based ILs combined with fluorinated anions. Although we also observe this behavior for the ILs with the most hydrophobic anions, namely $[BF_4]^-$ and $[B(CN)_4]^-$, an opposite pattern is verified with the remaining and more "hydrophilic" cyano-functionalized ILs. For more hydrophilic anions and where cation–anion interactions are also stronger, the higher refractive indices occur for short chain ILs. Indeed, we had already reported on this trend making use of acetate-based ILs.[54] In addition, the anion dependence of the refractive index is stronger than the cation alkyl side chain length dependence as shown in Figure 9.

At any temperature interval, any value of $n_D$ at a specific temperature can be estimated using the following equation,

$$n_D(T/K) = n_D(298.15\ K) + \partial n_D/\partial T(T/K - 298.15\ K)$$
(13)

where $n_D$ (298.15 K) is the refractive index at 298.15 K, and $\partial n_D/\partial T$ is the temperature derivative of the refractive index.

The derived refractive indices of all the studied ILs, at $T = 298.15$ K, are compiled in Table 7 along with the observed

**Table 7. Derived Refractive Index of the Studied ILs at 298.15 K, Corresponding Temperature Derivative, and Calculated Molar Refractions and Free Volumes**

| ionic liquid | $n_D$ | $10^4 \times (\partial n_D/\partial T)/K^{-1}$ | $R_m/(cm^3 \cdot mol^{-1})$ | $f_m/(cm^3 \cdot mol^{-1})$ |
|---|---|---|---|---|
| $[C_2C_1im][SCN]$ | 1.5506 | −3.30 | 48.32 | 103.20 |
| $[C_4C_1im][SCN]$ | 1.5394 | −3.07 | 57.83 | 126.65 |
| $[C_2C_1im][N(CN)_2]$ | 1.5112 | −3.27 | 48.10 | 112.41 |
| $[C_4C_1im][N(CN)_2]$ | 1.5080 | −3.70 | 57.71 | 135.88 |
| $[C_6C_1im][N(CN)_2]$ | 1.5039 | −3.38 | 67.14 | 159.62 |
| $[C_2C_1im][C(CN)_3]$ | 1.5124 | −3.62 | 55.84 | 130.15 |
| $[C_4C_1im][C(CN)_3]$ | 1.5065 | −3.50 | 65.08 | 153.80 |
| $[C_2C_1im][B(CN)_4]$ | 1.4469 | −3.48 | 58.28 | 159.89 |
| $[C_6C_1im][B(CN)_4]$ | 1.4526 | −3.37 | 76.90 | 207.84 |
| $[C_2C_1im][BF_4]$ | 1.4145 | −2.62 | 38.59 | 115.68 |
| $[C_4C_1im][BF_4]$ | 1.4217 | −2.62 | 47.77 | 140.32 |

data. Several equations have been proposed to calculate the molar refraction or molar polarizability making use of density and refractive index data.[55] An implication of some of these approaches is that the refractive index of a substance is higher when its molecules are more tightly packed, i.e., when the compound is denser. It should be remarked that Tariq et al.[55] observed an inverse dependency between the densities and refractive indices for the series of 1-alkyl-3-methylimidazolium bis(trifluoromethylsulfonyl)imide ILs. In this context, care must be taken when generalizing some relationships commonly employed to isotropic fluids since the nanostructure of ILs may hamper their application.[55] Despite these concerns, the derived molar refractions, $R_m$, and the free volumes, $f_m$, were additionally calculated according to eqs 14 and 15, respectively,

$$R_m = \frac{(n_D)^2 - 1}{(n_D)^2 + 2} \times \frac{M_w}{\rho}$$
(14)

$$f_m = V_m - R_m$$
(15)

where $M_w$ is the IL molecular weight, and $V_m$ is the respective molar volume.

The calculated $R_m$ and $f_m$ at 298.15 K and for each IL are displayed in Table 7.

Molar refraction is a measure of the total polarizability of a mole of a substance. In all examples, an increase in the cation alkyl side chain length led to an increase in the molar refraction as well as to a free volume increment, as expected.

The derived molar refractions and the free volumes as a function of the cyano-based anion are depicted in Figure 10.
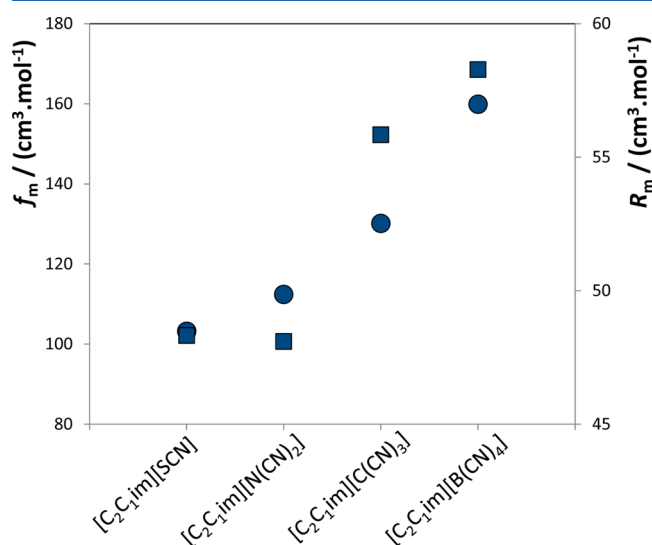


**Figure 10.** Free volume (●) and molar refraction (■) of $[C_2mim]$-based ILs at 298.15 K.

temperature derivative of the refractive index. The temperature dependence of the refractive index of each IL is very small; yet, it depends on the nature of the IL. A decrease in the refractive index of $(2.6\ to\ 3.6) \times 10^{-4}$ per K was observed for all ILs, which is less pronounced than that verified with common molecular solvents (ca. $4.5 \times 10^{-4}$ per K).[62]

To gather further insights into the intermolecular forces and behavior in solution of the selected ILs, the molar refractions can be also determined from the volumetric and refractive index

As clearly shown in Figure 10, the free volumes of the ILs increase in a quasi-linear trend with the number of cyano groups present at the anion. Nevertheless, molar refraction increases in the order $[N(CN)_2]^- < [SCN]^- < [C(CN)_3]^- < [B(CN)_4]^-$. The molar refraction does not strictly depend on the number of −CN groups present at the anion and the higher molar refraction values occur with the $[B(CN)_4]$-based fluids.

The contribution of each −CN-based anion on the refractive index of ILs was also identified using the group contribution

method proposed by Gardas and Coutinho,[52] which follows a linear function of the form,

$$n_D = A_{n_D} - B_{n_D} T \tag{16}$$

where

$$A_{n_D} = \sum_{i=1}^{k} n_i a_{i,n_D} \tag{17}$$

$$B_{n_D} = \sum_{i=1}^{k} n_i b_{i,n_D} \tag{18}$$

and where $n_i$ is the number of groups of type $i$, and $k$ is the total number of different groups in the molecule.

The new group contribution parameters, $a_{i,nD}$ and $b_{i,nD}$, for the cyano-containing anions are given in Table 8. These values

**Table 8. Group Contribution Parameters, $a_{i,\eta}$ and $b_{i,\eta}$, of the Group Contribution Method for the Prediction of Refractive Index According to the Gardas and Coutinho Model[52]**

| ionic species | $a_{i,\eta}$ | $b_{i,\eta}$ / K |
|---|---|---|
| | Cation[52] | |
| $[C_1C_1im]^+$ | 1.4436 | $2.268 \times 10^{-4}$ |
| | Anions | |
| $[SCN]^-$ | 0.1825 | $5.489 \times 10^{-5}$ |
| $[N(CN)_2]^-$ | 0.1612 | $1.384 \times 10^{-4}$ |
| $[C(CN)_3]^-$ | 0.1087 | $1.200 \times 10^{-4}$ |
| $[B(CN)_4]^-$ | 0.0572 | $1.104 \times 10^{-4}$ |
| | Additional Group[52] | |
| $-CH_2$ | 0.0353 | $7.330 \times 10^{-5}$ |

were estimated using our data in combination with that of the literature.[22,23,25,33,46] The predictive description of the refractive indices using eqs 16 to 18 is depicted in Figure 7. A maximum relative deviation of 0.91% was found. Nevertheless, due to the odd behavior observed experimentally with the most hydrophilic anions and the reverse trend in the refractive indices along the cation alkyl side chain, these divergences are reflected in the model predictions that follow the "common" pattern: higher refractive indices are observed with ILs with longer aliphatic moieties.

Finally, and making use of the predictive ability of the Gardas and Coutinho models,[51,52] Table 9 presents a summary of the thermophysical properties for the complete matrix of the $[C_nC_1im]$-cyano-based ILs ($2 \leq n \leq 6$).

## CONCLUSIONS

In line with the continual IL investigations, the knowledge of their thermophysical properties and the construction of a proper databank are essential requisites for the design of related industrial processes. Indeed, the study of the physicochemical properties and the structure−property relationships of ILs can potentially aid in the design of future applications. Therefore, in this work, we reported several physicochemical properties, namely density, viscosity, and refractive index, and their dependence on temperature, for a variety of imidazolium-based ILs containing cyano-functionalized anions. Specifically, we compared all the properties as a function of the alkyl side chain length of the imidazolium cation and according to the cyano-incorporating anion—$[SCN]^-$, $[N(CN)_2]^-$, $[C(CN)_3]^-$ and $[B(CN)_4]^-$—to provide a comprehensive analysis making use of structural considerations.

**Table 9. Predictive Properties Values at 298.15 K, for All the ILs in the Matrix, Using the Models Proposed by Gardas and Coutinho[51,52]**

| IL | $\rho/(kg \cdot m^{-3})$ | $\eta/(mPa \cdot s)$ | $n_D$ |
|---|---|---|---|
| $[C_2C_1im][SCN]$ | 1121.1 | 24.564 | 1.55556 |
| $[C_4C_1im][SCN]$ | 1068.5 | 39.081 | 1.58245 |
| $[C_6C_1im][SCN]$ | 1032.2 | 62.178 | 1.60934 |
| $[C_2C_1im][N(CN)_2]$ | 1107.6 | 18.874 | 1.50936 |
| $[C_4C_1im][N(CN)_2]$ | 1059.8 | 30.028 | 1.53625 |
| $[C_6C_1im][N(CN)_2]$ | 1026.2 | 47.774 | 1.56314 |
| $[C_2C_1im][C(CN)_3]$ | 1086.3 | 17.346 | 1.46235 |
| $[C_4C_1im][C(CN)_3]$ | 1047.3 | 27.597 | 1.48924 |
| $[C_6C_1im][C(CN)_3]$ | 1018.7 | 43.907 | 1.51613 |
| $[C_2C_1im][B(CN)_4]$ | 1035.3 | 19.313 | 1.41371 |
| $[C_4C_1im][B(CN)_4]$ | 1008.3 | 30.727 | 1.44060 |
| $[C_6C_1im][B(CN)_4]$ | 987.6 | 48.886 | 1.46749 |

Our data allowed us to conclude that for density, and independently of the cation, the values decrease with an increase in the number of cyano groups from the $[SCN]-$ to the $[B(CN)_4]$-based fluids and closely correlate with the anions' molecular weight. Moreover, particularly high refractive indices were observed for the thiocyanate-based ILs, suggesting their potential applicability as optical materials. In general, the refractive indices were found to decrease according to the rank: $[SCN]^- > [N(CN)_2]^- \approx [C(CN)_3]^- > [B(CN)_4]^-$. Finally, the trend obtained for viscosity was not straightforward and did not depend on the number of −CN groups at the anion. The viscosity of the cyano-based ILs decreased in the order: $[SCN]^- > [B(CN)_4]^- > [N(CN)_2]^- > [C(CN)_3]^-$. Tricyano-methane-based fluids had exceptionally low viscosities and are among the most desirable ILs for industrial applications.

The isobaric thermal expansion coefficient, the derived molar refraction, the free volume and the energy barrier on viscosity of all compounds were calculated based on the experimental data and were presented and discussed.

The Gardas and Coutinho group contribution models were also applied to the three measured properties, and new group contribution parameters were proposed. The novel groups promise to usefully predict the properties of ILs as yet experimentally characterized.

## ■ ASSOCIATED CONTENT

**ⓢ Supporting Information**

Tables reporting the experimental data, and figures with the comparison between the experimental results obtained in this work and literature data. This material is available free of charge via the Internet at http://pubs.acs.org.

## ■ AUTHOR INFORMATION

**Corresponding Author**

*E-mail: maragfreire@ua.pt; Tel: +351 234370200; Fax: +351 234370084.

**Notes**

The authors declare no competing financial interest.

## ■ REFERENCES

(1) Plechkova, N. V.; Seddon, K. R. Applications of Ionic Liquids in the Chemical Industry. *Chem. Soc. Rev.* **2008**, *37*, 123–150.

(2) Tokuda, H.; Hayamizu, K.; Ishii, K.; Susan, A. B. H.; Watanabe, M. Physicochemical Properties and Structures of Room Temperature Ionic Liquids. 1. Variation of Anionic Species. *J. Phys. Chem. B* **2004**, *108*, 16593–16600.

(3) Tariq, M.; Carvalho, P. J.; Coutinho, J. A. P.; Marrucho, I. M.; Canongia Lopes, J. N.; Rebelo, L. P. N. Viscosity of $(C_2-C_{14})$ 1-Alkyl-3-methylimidazolium Bis(trifluoromethylsulfonyl)amide Ionic Liquids in an Extended Temperature Range. *Fluid Phase Equilib.* **2011**, *301*, 22–32.

(4) Oliveira, F. S.; Freire, M. G.; Carvalho, P. J.; Coutinho, J. A. P.; Canongia Lopes, J. N.; Rebelo, L. P. N.; Marrucho, I. M. Structural and Positional Isomerism Influence in the Physical Properties of Pyridinium $NTf_2$-Based Ionic Liquids: Pure and Water-Saturated Mixtures. *J. Chem. Eng. Data* **2010**, *55*, 4514–4520.

(5) MacFarlane, D. R.; Golding, J.; Forsyth, S.; Forsyth, M.; Deacon, G. B. Low Viscosity Ionic Liquids Based on Organic Salts of the Dicyanamide Anion. *Chem. Commun.* **2001**, 1430–1431.

(6) Kuang, D.; Wang, P.; Ito, S.; Zakeeruddin, S. M.; Grätzel, M. Organic Dye-Sensitized Ionic Liquid Based Solar Cells: Remarkable Enhancement in Performance through Molecular Design of Indoline Sensitizers. *J. Am. Chem. Soc.* **2006**, *128*, 7732–7733.

(7) Scheers, J.; Johansson, P.; Jacobsson, P. Anions for Lithium Battery Electrolytes: A Spectroscopic and Theoretical Study of the $B(CN)_4^-$ Anion of the Ionic Liquid $C_2mim[B(CN)_4]$. *J. Electrochem. Soc.* **2008**, *155*, A628–A634.

(8) Zhou, D.; Bai, Y.; Zhang, J.; Cai, N.; Su, M.; Wang, Y.; Zhang, M.; Wang, P. Anion Effects in Organic Dye-Sensitized Mesoscopic Solar Cells with Ionic Liquid Electrolytes: Tetracyanoborate vs Dicyanamide. *J. Phys. Chem. C* **2011**, *115*, 816–822.

(9) Marszalek, M.; Fei, Z.; Zhu, D.-R.; Scopelliti, R.; Dyson, P. J.; Zakeeruddin, S. M.; Grätzel, M. Application of Ionic Liquids Containing Tricyanomethanide $[C(CN)_3]^-$ or Tetracyanoborate $[B(CN)_4]^-$ Anions in Dye-Sensitized Solar Cells. *Inorg. Chem.* **2011**, *50*, 11561–11567.

(10) Mahurin, S. M.; Lee, J. S.; Baker, J. A.; Luo, H.; Dai, S. Performance of Nitrile-Containing Anions in Task-Specific Ionic Liquids for Improved $CO_2/N_2$ Separation. *J. Membr. Sci.* **2010**, *353*, 177–183.

(11) Twu, P.; Zhao, Q.; Pitner, W. R.; Acree, W. E.; Baker, G. A.; Anderson, J. L. Evaluating the Solvation Properties of Functionalized Ionic Liquids with Varied Cation/Anion Composition Using the Solvation Parameter Model. *J. Chromatogr. A* **2011**, *1218*, 5311–5318.

(12) Heitmann, S.; Krings, J.; Kreis, P.; Lennert, A.; Pitner, W. R.; Górak, A.; Schulte, M. M. Recovery of *n*-Butanol using Ionic Liquid-Based Pervaporation Membranes. *Sep. Purif. Technol.* **2012**, *97*, 108–114.

(13) Neves, C. M. S. S.; Granjo, J. F. O.; Freire, M. G.; Robertson, A.; Oliveira, N. M. C.; Coutinho, J. A. P. Separation of Ethanol–Water Mixtures by Liquid–Liquid Extraction using Phosphonium-Based Ionic Liquids. *Green Chem.* **2011**, *13*, 1517–1526.

(14) Meindersma, G. W.; Hansmeier, A. R.; de Haan, A. B. Cyano-Containing Ionic Liquids for the Extraction of Aromatic Hydrocarbons from an Aromatic/Aliphatic Mixture. *Ind. Eng. Chem. Res.* **2010**, *49*, 7530–7540.

(15) Cláudio, A. F. M.; Freire, M. G.; Freire, C. S. R.; Silvestre, A. J. D.; Coutinho, J. A. P. Extraction of Vanillin Using Ionic-Liquid-Based Aqueous Two-Phase Systems. *Sep. Purif. Technol.* **2010**, *75*, 39–47.

(16) Conceição, L. J. A.; Bogel-Łukasik, E.; Bogel-Łukasik, R. A New Outlook on Solubility of Carbohydrates and Sugar Alcohols in Ionic Liquids. *RSC Adv.* **2012**, *2*, 1846–1855.

(17) Mota-Martinez, M. T.; Althuluth, M.; Kroon, M. C.; Peters, C. J. Solubility of Carbon Dioxide in the Low-Viscosity Ionic Liquid 1-Hexyl-3-methylimidazolium Tetracyanoborate. *Fluid Phase Equilib.* **2012**, *332*, 35–39.

(18) Carvalho, P. J.; Regueira, T.; Santos, L. M. N. B. F.; Fernandez, J.; Coutinho, J. A. P. Effect of Water on the Viscosities and Densities of 1-Butyl-3-methylimidazolium Dicyanamide and 1-Butyl-3-methylimidazolium Tricyanomethane at Atmospheric Pressure. *J. Chem. Eng. Data* **2010**, *55*, 645–652.

(19) Domańska, U.; Królikowska, M.; Królikowski, M. Phase Behaviour and Physico-Chemical Properties of the Binary Systems {1-Ethyl-3-methylimidazolium Thiocyanate, or 1-Ethyl-3-methylimidazolium Tosylate + Water, or + an Alcohol}. *Fluid Phase Equilib.* **2010**, *294*, 72–83.

(20) Ficke, L. E.; Novak, R. R.; Brennecke, J. F. Thermodynamic and Thermophysical Properties of Ionic Liquid + Water Systems. *J. Chem. Eng. Data* **2010**, *55*, 4946–4950.

(21) Fredlake, C. P.; Crosthwaite, J. M.; Hert, D. G.; Aki, S. N. V. K.; Brennecke, J. F. Thermophysical Properties of Imidazolium-based Ionic Liquids. *J. Chem. Eng. Data* **2004**, *49*, 954–964.

(22) Freire, M. G.; Teles, A. R. R.; Rocha, M. A. A.; Schröder, B.; Neves, C. M. S. S.; Carvalho, P. J.; Evtuguin, D. V.; Santos, L. M. N. B. F.; Coutinho, J. A. P. Thermophysical Characterization of Ionic Liquids Able To Dissolve Biomass. *J. Chem. Eng. Data* **2011**, *56*, 4813–4822.

(23) Fröba, A. P.; Kremer, H.; Leipertz, A. Density, Refractive Index, Interfacial Tension, and Viscosity of Ionic Liquids $[EMIM][EtSO_4]$, $[EMIM][NTf_2]$, $[EMIM][N(CN)_2]$, and $[OMA][NTf_2]$ in Dependence on Temperature at Atmospheric Pressure. *J. Phys. Chem. B* **2008**, *112*, 12420–12430.

(24) Klomfar, J.; Součková, M.; Pátek, J. Temperature Dependence of the Surface Tension and Density at 0.1 MPa for 1-Ethyl- and 1-Butyl-3-methylimidazolium Dicyanamide. *J. Chem. Eng. Data* **2011**, *56*, 3454–3462.

(25) Koller, T.; Rausch, M. H.; Schulz, P. S.; Berger, M.; Wasserscheid, P.; Economou, I. G.; Leipertz, A.; Fröba, A. P. Viscosity, Interfacial Tension, Self-Diffusion Coefficient, Density, and Refractive Index of the Ionic Liquid 1-Ethyl-3-methylimidazolium Tetracyanoborate as a Function of Temperature at Atmospheric Pressure. *J. Chem. Eng. Data* **2012**, *57*, 828–835.

(26) Królikowska, M.; Hofman, T. Densities, Isobaric Expansivities and Isothermal Compressibilities of the Thiocyanate-Based Ionic Liquids at Temperatures (298.15–338.15 K) and Pressures up to 10 MPa. *Thermochim. Acta* **2012**, *530*, 1–6.

(27) Meindersma, G. W.; Simons, B. T. J.; de Haan, A. B. Physical Properties of 3-Methyl-*N*-butylpyridinium Tetracyanoborate and 1-Butyl-1-methylpyrrolidinium Tetracyanoborate and Ternary LLE Data of $[3\text{-mebupy}]B(CN)_4$ with an Aromatic and an Aliphatic Hydrocarbon at $T = 303.2$ and 328.2 K and p = 0.1 MPa. *J. Chem. Thermodyn.* **2011**, *43*, 1628–1640.

(28) Neves, C. M. S. S.; Carvalho, P. J.; Freire, M. G.; Coutinho, J. A. P. Thermophysical Properties of Pure and Water-Saturated Tetradecyltrihexylphosphonium-Based Ionic Liquids. *J. Chem. Thermodyn.* **2011**, *43*, 948–957.

(29) Pereiro, A. B.; Veiga, H. I. M.; Esperança, J. M. S. S.; Rodríguez, A. Effect of Temperature on the Physical Properties of Two Ionic Liquids. *J. Chem. Thermodyn.* **2009**, *41*, 1419–1423.

(30) Quijada-Maldonado, E.; van der Boogaart, S.; Lijbers, J. H.; Meindersma, G. W.; de Haan, A. B. Experimental Densities, Dynamic Viscosities and Surface Tensions of the Ionic Liquids Series 1-Ethyl-3-methylimidazolium Acetate and Dicyanamide and their Binary and Ternary Mixtures with Water and Ethanol at $T$ = (298.15 to 343.15 K). *J. Chem. Thermodyn.* **2012**, *51*, 51–58.

(31) Sánchez, L. G.; Espel, J. R.; Onink, F.; Meindersma, G. W.; de Haan, A. B. Density, Viscosity, and Surface Tension of Synthesis Grade

10282

dx.doi.org/10.1021/jp405913b | *J. Phys. Chem. B* 2013, 117, 10271–10283

Imidazolium, Pyridinium, and Pyrrolidinium Based Room Temperature Ionic Liquids. *J. Chem. Eng. Data* **2009**, *54*, 2803−2812.

(32) Schreiner, C.; Zugmann, S.; Hartl, R.; Gores, H. J. Fractional Walden Rule for Ionic Liquids: Examples from Recent Measurements and a Critique of the So-Called Ideal KCl Line for the Walden Plot. *J. Chem. Eng. Data* **2010**, *55*, 1784−1788.

(33) Seoane, R. G.; Corderí, S.; Gómez, E.; Calvar, N.; González, E. J.; Macedo, E. A.; Domínguez, Á. Temperature Dependence and Structural Influence on the Thermophysical Properties of Eleven Commercial Ionic Liquids. *Ind. Eng. Chem. Res.* **2012**, *51*, 2492−2504.

(34) Tong, J.; Liu, Q.-S.; Kong, Y.-X.; Fang, D.-W.; Welz-Biermann, U.; Yang, J.-Z. Physicochemical Properties of an Ionic Liquid [C₂mim][B(CN)₄]. *J. Chem. Eng. Data* **2010**, *55*, 3693−3696.

(35) Wong, C.-L.; Soriano, A. N.; Li, M.-H. Diffusion Coefficients and Molar Conductivities in Aqueous Solutions of 1-Ethyl-3-methylimidazolium-Based Ionic Liquids. *Fluid Phase Equilib.* **2008**, *271*, 43−52.

(36) Domańska, U.; Królikowska, M. Density and Viscosity of Binary Mixtures of {1-Butyl-3-methylimidazolium Thiocyanate + 1-Heptanol, 1-Octanol, 1-Nonanol, or 1-Decanol}. *J. Chem. Eng. Data* **2010**, *55*, 2994−3004.

(37) Guerrero, H.; Martín, S.; Pérez-Gregorio, V.; Lafuente, C.; Bandrés, I. Volumetric Characterization of Pyridinium-Based Ionic Liquids. *Fluid Phase Equilib.* **2012**, *317*, 102−109.

(38) Ziyada, A. K.; Wilfred, C. D.; Murugesan, T. Densities, Viscosities and Refractive Indices of 1-Alkyl-3-propanenitrile Imidazolium Chloride Ionic Liquids. *Phys. Chem. Liq.* **2012**, *50*, 152−160.

(39) Ziyada, A. K.; Bustam, M. A.; Wilfred, C. D.; Murugesan, T. Densities, Viscosities, and Refractive Indices of 1-Hexyl-3-propanenitrile Imidazolium Ionic Liquids Incorporated with Sulfonate-Based Anions. *J. Chem. Eng. Data* **2011**, *56*, 2343−2348.

(40) Ziyada, A. K.; Wilfred, C. D.; Bustam, M. A.; Man, Z.; Murugesan, T. Thermophysical Properties of 1-Propyronitrile-3-alkylimidazolium Bromide Ionic Liquids at Temperatures from (293.15 to 353.15) K. *J. Chem. Eng. Data* **2010**, *55*, 3886−3890.

(41) Yoshida, Y.; Muroi, K.; Otsuka, A.; Saito, G.; Takahashi, M.; Yoko, T. 1-Ethyl-3-methylimidazolium Based Ionic Liquids Containing Cyano Groups: Synthesis, Characterization, and Crystal Structure. *Inorg. Chem.* **2004**, *43*, 1458−1462.

(42) Stoppa, A.; Hunger, J.; Buchner, R. Conductivities of Binary Mixtures of Ionic Liquids with Polar Solvents. *J. Chem. Eng. Data* **2009**, *54*, 472−479.

(43) Gardas, R. L.; Freire, M. G.; Carvalho, P. J.; Marrucho, I. M.; Fonseca, I. M. A.; Ferreira, A. G. M.; Coutinho, J. A. P. PρT Measurements of Imidazolium-Based Ionic Liquids. *J. Chem. Eng. Data* **2007**, *52*, 1881−1888.

(44) Xing, D. Y.; Peng, N.; Chung, T.-S. Formation of Cellulose Acetate Membranes via Phase Inversion Using Ionic Liquid, [BMIM]SCN, As the Solvent. *Ind. Eng. Chem. Res.* **2010**, *49*, 8761−8769.

(45) Sánchez, L. G.; Espel, J. R.; Onink, F.; Meindersma, G. W.; de Haan, A. B. Density, Viscosity, and Surface Tension of Synthesis Grade Imidazolium, Pyridinium, and Pyrrolidinium Based Room Temperature Ionic Liquids. *J. Chem. Eng. Data* **2009**, *54*, 2803−2812.

(46) Seki, S.; Tsuzuki, S.; Hayamizu, K.; Umebayashi, Y.; Serizawa, N.; Takei, K.; Miyashiro, H. Comprehensive Refractive Index Property for Room-Temperature Ionic Liquids. *J. Chem. Eng. Data* **2012**, *57*, 2211−2216.

(47) Zech, O.; Stoppa, A.; Buchner, R.; Kunz, W. The Conductivity of Imidazolium-Based Ionic Liquids from (248 to 468) K. B. Variation of the Anion. *J. Chem. Eng. Data* **2010**, *55*, 1774−1778.

(48) Mahurin, S. M.; Lee, J. S.; Baker, G. A.; Luo, H.; Dai, S. Performance of Nitrile-Containing Anions in Task-Specific Ionic Liquids for Improved CO₂/N₂ Separation. *J. Membr. Sci.* **2010**, *353*, 177−183.

(49) Rosol, Z. P.; German, N. J.; Gross, S. M. Solubility, Ionic Conductivity and Viscosity of Lithium Salts in Room Temperature Ionic Liquids. *Green Chem.* **2009**, *11*, 1453−1457.

(50) Sterner, E. S.; Rosol, Z. P.; Gross, E. M.; Gross, S. M. Thermal Analysis and Ionic Conductivity of Ionic Liquid Containing Composites with Different Crosslinkers. *J. Appl. Polym. Sci.* **2009**, *114*, 2963−2970.

(51) Gardas, R. L.; Coutinho, J. A. P. Extension of the Ye and Shreeve Group Contribution Method for Density Estimation of Ionic Liquids in a Wide Range of Temperatures and Pressures. *Fluid Phase Equilib.* **2008**, *263*, 26−32.

(52) Gardas, R. L.; Coutinho, J. A. P. Group Contribution Methods for the Prediction of Thermophysical and Transport Properties of Ionic Liquids. *AIChE J.* **2009**, *55*, 1274−1290.

(53) Almeida, H. F. D.; Lopes-da-Silva, J. A.; Freire, M. G.; Coutinho, J. A. P. Surface Tension and Refractive Index of Pure and Water-Saturated Tetradecyltrihexylphosphonium-Based Ionic Liquids. *J. Chem. Thermodyn.* **2013**, *57*, 372−379.

(54) Almeida, H. F. D.; Passos, H.; Lopes-da-Silva, J. A.; Fernandes, A. M.; Freire, M. G.; Coutinho, J. A. P. Thermophysical Properties of Five Acetate-Based Ionic Liquids. *J. Chem. Eng. Data* **2012**, *57*, 3005−3013.

(55) Tariq, M.; Forte, P. A. S.; Gomes, M. F. C.; Canongia Lopes, J. N.; Rebelo, L. P. N. Densities and Refractive Indices of Imidazolium- and Phosphonium-Based Ionic Liquids: Effect of Temperature, Alkyl Chain Length, and Anion. *J. Chem. Thermodyn.* **2009**, *41*, 790−798.

(56) Gardas, R. L.; Freire, M. G.; Carvalho, P. J.; Marrucho, I. M.; Fonseca, I. M. A.; Ferreira, A. G. M.; Coutinho, J. A. P. High-Pressure Densities and Derived Thermodynamic Properties of Imidazolium-Based Ionic Liquids. *J. Chem. Eng. Data* **2007**, *52*, 80−88.

(57) Tariq, M.; Serro, A. P.; Saramago, B.; Esperança, J. M. S. S.; Canongia Lopes, J. N.; Rebelo, L. P. N. High-Temperature Surface Tension and Density Measurements of 1-Alkyl-3-methylimidazolium Bistriflamide Ionic Liquids. *Fluid Phase Equilib.* **2010**, *294*, 131−138.

(58) Esperança, J. M. S. S.; Guedes, H. J. R.; Blesic, M.; Rebelo, L. P. N. Densities and Derived Thermodynamic Properties of Ionic Liquids. 3. Phosphonium-Based Ionic Liquids over an Extended Pressure Range. *J. Chem. Eng. Data* **2006**, *51*, 237−242.

(59) Blesic, M.; Swadźba-Kwaśny, M.; Belhocine, T.; Gunaratne, H. Q. N.; Canongia Lopes, J. N.; Gomes, M. F. C.; Pádua, A. A. H.; Seddon, K. R.; Rebelo, L. P. N. 1-Alkyl-3-methylimidazolium Alkanesulfonate Ionic Liquids, [CₙH₂ₙ₊₁mim][CₖH₂ₖ₊₁SO₃]: Synthesis and Physicochemical Properties. *Phys. Chem. Chem. Phys.* **2009**, *11*, 8939−8948.

(60) Kolbeck, C.; Cremer, T.; Lovelock, K. R. J.; Paape, N.; Schulz, P. S.; Wasserscheid, P.; Maier, F.; Steinrück, H. P. Influence of Different Anions on the Surface Composition of Ionic Liquids Studied Using ARXPS. *J. Phys. Chem. B* **2009**, *113*, 8682−8688.

(61) Ye, C.; Shreeve, J. M. Rapid and Accurate Estimation of Densities of Room Temperature Ionic Liquids and Salts. *J. Phys. Chem. A* **2007**, *111*, 1456−1461.

(62) NIST Chemistry Webbook at http://webbook.nist.gov/chemistry/.

(63) Grunberg, L.; Nissan, A. H. Mixture Law for Viscosity. *Nature* **1949**, *164*, 799−800.

10283

dx.doi.org/10.1021/jp405913b | *J. Phys. Chem. B* 2013, 117, 10271−10283